# Nonlinear Dynamics of Random Surface Gravity Waves Over Water of Slowly Varying Depth

A. Perelomova*

*Gdansk University of Technology, Faculty of Applied Physics and Mathematics, 11/12 Gabriela Narutowicza Street, 80-233 Gdańsk, Poland*

Received: 10.09.2025 & Accepted: 04.03.2026

Doi: 10.12693/APhysPolA.149.97 *e-mail: anna.perelomova@pg.edu.pl

The weakly nonlinear propagation of a random surface wave over a water region of varying depth $h$ is considered. A random, stationary Gaussian process describing perturbations in the volume of the liquid is assumed at infinite depth. The characteristics of the nonlinear random wave are evaluated as the wave propagates into shallow coastal waters. It is found that the mean amplitude of the fundamental harmonic of the wave is proportional to $h^{7/8}$, while its variance is proportional to $h^{7/4}$ as the wave approaches the coastal zone. The mean amplitude of the second harmonic is proportional to $h^{-1/4}$. Manifestation of nonlinear effects becomes abrupt when the water depth falls below a certain critical value. This behavior occurs for relatively small energy densities of the perturbation at infinite depth, as specified in the study. For larger energy densities, nonlinear effects increase gradually.

topics: dispersive media, nonlinear dynamics, surface gravity waves, random Gaussian process

## 1. Introduction

The first fully modern theory of surface waves was developed in 1841 by G.B. Airy [1], who used of a linear approximation for small-amplitude waves and derived the dispersion relation connecting wave period, wavelength, and water depth. G.G. Stokes [2] extended Airy's theory to describe finite-amplitude waves. Stokes' theory explained nonlinear phenomena in wave dynamics, such as crest sharpening, wave steepening, and excitation of higher harmonics. Another important achievement was the development of the theory of solitary and long waves, with the Korteweg-de Vries (KdV) equation derived by Korteweg and de Vries [3] in 1895, which mathematically captures solitary waves and predicts stationary solitons.

The modern era of surface–wave research focuses on wind-wave generation, turbulent flows, and shear-flow instability theory [4, 5]. Contemporary surface–wave theory incorporates nonlinear dynamics and numerical simulations. The transformation of surface gravity waves during propagation into shallow coastal waters is a fundamental problem in physical oceanography, coastal engineering, and nearshore morphodynamics. Among the most prominent transformation processes is wave shoaling, that is, the increase in wave height that occurs when wave energy is compressed into a water column of decreasing depth [6, 7]. Classical linear wave theory provides a first-order description of shoaling by the conservation of wave energy flux as waves encounter gradually varying bathymetry [8]. However, wave shoaling in natural environments is almost always nonlinear.

Nonlinear effects include amplitude dispersion, bound harmonics, and triad interactions. These effects become increasingly significant as waves enter transitional and shallow depths, leading to wave asymmetry, spectral energy transfer, and ultimately wave breaking. Linear theory is valid only when the velocity is small compared to the wave phase speed [9]. The dynamics of surface gravity waves are determined by equations with nonlinear boundary conditions, making the mathematical description of finite-amplitude wave dynamics particularly challenging. Modern numerical frameworks, such as high-resolution computational fluid dynamics (CFD), have enabled more accurate treatment of these nonlinearities (e.g., [10]). The current state of knowledge of wave dynamics in basins is fairly advanced. A tremendous number of theoretical studies, along with advances in numerical methods, allow for consideration of a wide variety of practically important problems; nevertheless, interest in the nonlinear dynamics of surface gravity waves continues to grow.

This study examines the dynamics of random surface gravity waves using a theoretical approach. The analysis relies on simplified equations derived from conservation laws and boundary conditions. A random Gaussian process at infinite depth is considered, representing the superposition of independent random processes far from the coastal zone. This assumption appears reasonable, given the many factors that influence surface perturbations in deep water. The main advantage of the present study lies in its simplicity. It does not attempt to account for complex evolutionary factors, but instead provides a qualitative and quantitative analysis of the development of nonlinear effects as waves propagate to shallow depths.

The study is based on simple and physically reasonable ideas commonly applied in perturbation theory to describe the nonlinear dynamics of random waves. This requires the introduction of a generic small parameter characterizing the motion. The next step is to seek solutions of the approximate equations in the form of a series expansion in powers of this small parameter. Despite simplifying assumptions, the theory remains valid over a wide range of water depths, provided that the depth varies slowly with the horizontal coordinate and that the energy of the perturbations at infinite depth spans a sufficiently large domain. This approach makes it possible to draw conclusions about the rapid development of nonlinear behavior beginning at a certain critical depth, which depends on the dimensionless wave energy far from the coastal zone. This energy, in turn, depends on the magnitude and frequency of the perturbations. The paper provides numerical estimates of this critical depth.

## 2. Small-magnitude perturbations of the free surface

The mathematical analysis of surface waves refers to the solution of hydrodynamic equations describing the motion of an ideal, inviscid, incompressible fluid. These are the momentum equation (the modified second law of Newton) and the continuity equation (conservation of mass in differential form), respectively, given by

$$\frac{\partial \boldsymbol{v}}{\partial t} + (\boldsymbol{v}\cdot\nabla)\boldsymbol{v} + \frac{1}{\rho}\nabla p = \boldsymbol{g} \quad \text{and} \quad \nabla\cdot\boldsymbol{v} = 0, \tag{1}$$

where $\rho$ is the liquid density, $\boldsymbol{v}$ denotes the velocity of liquid's particles, $p$ is the pressure, and $\boldsymbol{g}$ is the gravitational acceleration (e.g., [9, 11]). Two-dimensional flow in Cartesian coordinates $x$ (horizontal) and $z$ is considered ($z = 0$ corresponds to an unperturbed surface). The equations in (1) must be supplemented with boundary conditions. One of these expresses the requirement that the fluid particles do not detach from the bottom of variable depth $z = -h(x)$. Dynamic and kinematic conditions should be satisfied at the free boundary

$$p = p_0, \quad \frac{\mathrm{d}\xi}{\mathrm{d}t} = \frac{\partial\xi}{\partial t} + (\boldsymbol{v}\cdot\nabla)\xi = v_z, \quad \text{if } z = \xi(x,t), \tag{2}$$

where $p_0$ is the atmospheric pressure, and $\xi(x,t)$ is the height of the surface wave measured from $z = 0$. The important case of flow refers to the potential field of velocity ($\nabla\times\boldsymbol{v} = 0$) with velocity potential $\Phi(x,z,t)$ ($\boldsymbol{v}\equiv\nabla\Phi$). We consider weak dependence of $h$ on $x$. Equations in (1) and the boundary conditions may be readily rearranged as

$$\begin{aligned}
&\Delta\Phi \equiv \frac{\partial^2\Phi}{\partial x^2} + \frac{\partial^2\Phi}{\partial z^2} = 0 && (-h<z<\xi(x,t)),\\
&\frac{\partial\Phi}{\partial x}\frac{\mathrm{d}h}{\mathrm{d}x} + \frac{\partial\Phi}{\partial z} = 0 && (z=-h(x)),\\
&g\xi + \frac{\partial\Phi}{\partial t} + \frac{1}{2}\Big[\Big(\frac{\partial\Phi}{\partial x}\Big)^2 + \Big(\frac{\partial\Phi}{\partial z}\Big)^2\Big] = 0 && (z=\xi(x,t)),\\
&\frac{\partial\xi}{\partial t} + \frac{\partial\Phi}{\partial x}\frac{\partial\xi}{\partial x} - \frac{\partial\Phi}{\partial z} = 0 && (z=\xi(x,t)).
\end{aligned} \tag{3}$$

The boundary conditions for $z = \xi(x,t)$ are nonlinear. We seek a solution to (3) by expanding in a power series in a small parameter $\varepsilon$ which equals the product of the amplitude of the surface disturbance $a$ and its wavenumber $k$, so $\varepsilon = a\,k$ (the validity of the results and the relevant set of small parameters are discussed in more detail in Sect. 2.3); thus

$$\Phi = \varepsilon\Phi_1 + \varepsilon^2\Phi_2, \qquad \xi = \varepsilon\xi_1 + \varepsilon^2\xi_2. \tag{4}$$

Collecting the leading-order terms, we arrive at

$$\Phi(x,\xi,t) = \varepsilon\Phi_1\Big|_{\xi=0} + \varepsilon^2\left(\xi_1\frac{\partial\Phi_1}{\partial z}|_{\xi=0} + \Phi_2|_{\xi=0}\right). \tag{5}$$

The equations in (3) take the leading-order forms

$$\begin{aligned}
&\Delta\Phi_1 = 0,\\
&\Delta\Phi_2 = 0,\\
&\frac{\partial\Phi_1}{\partial x}\frac{\mathrm{d}h}{\mathrm{d}x} + \frac{\partial\Phi_1}{\partial z} = 0 && (z=-h(x)),\\
&\frac{\partial\Phi_2}{\partial x}\frac{\mathrm{d}h}{\mathrm{d}x} + \frac{\partial\Phi_2}{\partial z} = 0 && (z=-h(x)),\\
&g\xi_1 + \frac{\partial\Phi_1}{\partial t} = 0 && (z=0),\\
&g\xi_2 + \frac{\partial\Phi_2}{\partial t} = -\frac{1}{2}\left[\Big(\frac{\partial\Phi_1}{\partial x}\Big)^2 + \Big(\frac{\partial\Phi_1}{\partial z}\Big)^2\right] - \xi_1\frac{\partial^2\Phi_1}{\partial z\partial t} && (z=0),\\
&\frac{\partial\xi_1}{\partial t} - \frac{\partial\Phi_1}{\partial z} = 0 && (z=0),\\
&\frac{\partial\xi_2}{\partial t} - \frac{\partial\Phi_2}{\partial z} = -\frac{\partial\Phi_1}{\partial x}\frac{\partial\xi_1}{\partial x} + \xi_1\frac{\partial^2\Phi_1}{\partial z^2} && (z=0).
\end{aligned} \tag{6}$$

Considering a weakly variable $h(x)$, one may use the leading-order boundary conditions

$$\frac{\partial \Phi_1}{\partial z} = 0, \quad \frac{\partial \Phi_2}{\partial z} = 0, \quad \text{if } z = -h(x). \tag{7}$$

In fact, we introduce two small parameters, $\varepsilon$ and maximum of $\frac{\mathrm{d}h}{\mathrm{d}x}$ over the domain of $x$, and consider them of the same order of smallness (see [12]).

### 2.1. Energy balance in the course of weakly nonlinear dynamics

The total energy in a volume $V$ with unit horizontal length perpendicular to the $x$ and $z$ directions, $V: x_0 \le x \le x_0 + \Delta x,\ -h(x) \le z \le \xi(x,t)$, consists of kinetic and potential contributions, so

$$E(x_0, \Delta x, t) = \frac{\rho}{2} \int_V \mathrm{d}V \left[ \left( \frac{\partial \Phi}{\partial x} \right)^2 + \left( \frac{\partial \Phi}{\partial z} \right)^2 \right] + \rho g \int_{x_0}^{x_0+\Delta x} \mathrm{d}x \int_{-h(x)}^{\xi(x,t)} \mathrm{d}z\ z. \tag{8}$$

At infinite depth, $h \to \infty$, the perturbation is assumed to be harmonic

$$\xi_1 = a \cos(\omega t - k\, x). \tag{9}$$

We treat the perturbation frequency $\omega$ as a constant. The depth $h$ is assumed to vary slowly with $x$, while the amplitude $a$ and the wavenumber $k$ are treated as functions of of $h$. The first- and second-order solutions are well established (see, e.g., [8, 9, 13]). The first- and second-order solutions satisfying the boundary conditions take the form

$$\begin{cases} \Phi_1 = -\dfrac{g\, a}{\omega} \dfrac{\cosh k(z+h)}{\cosh(k\, h)} \sin(\phi), \\ \Phi_2 = -\dfrac{3a^2\, \omega}{8} \dfrac{\cosh 2k(z+h)}{\sinh^4(k\, h)} \sin(2\phi), \\ \xi_2 = \dfrac{k^2\, a^2\, g}{4\omega^2} \left( 2 + \dfrac{3}{\sinh^2(k\, h)} \right) \cos(2\phi), \end{cases} \tag{10}$$

where $\phi = \omega t - kx$, and the dispersion relation connecting the frequency $\omega$ and the wave number $k$ is given by the well-known formula

$$\omega^2 = g\, k \tanh(k\, h). \tag{11}$$

Analytical formulas for the wave elevation and the potential function up to second order, describing the superposition of two waves of two-dimensional wave numbers, were derived by J.F. Dalzell [14]. In particular, Eq. (16) in [14] can be readily rearranged to (10), given in this paper, when one of the interacting wave amplitudes is set to zero in the case of a non-zero mean wave elevation. The first terms in the series expansion in powers of $\varepsilon$ of the energy density of a fluid element located at the horizontal coordinate $x$, $E_x = \frac{\partial E(x, \Delta x, t)}{\partial \Delta x}$, are

$$\frac{\partial E_x}{\partial t} = \varepsilon^2 \frac{\partial E^{(2)}}{\partial t} + \varepsilon^3 \frac{\partial E^{(3)}}{\partial t} + \varepsilon^4 \frac{\partial E^{(4)}}{\partial t} + \dots \tag{12}$$

Considering perturbations of constant frequency and magnitude given by (9), we conclude that the mean energies of the third and all odd orders vanish when averaged over the oscillation period; thus

$$\left\langle \frac{\partial E^{(3)}}{\partial t} \right\rangle = 0, \ \dots \tag{13}$$

The loss of the first harmonic energy is approximately equal to the increase in the energy of the second harmonic during weakly nonlinear dynamics. This energy transfer is expressed by the conservation equation [15]

$$\left\langle \frac{\partial E^{(2)}}{\partial t} \right\rangle + \left\langle \frac{\partial E^{(4)}}{\partial t} \right\rangle = 0, \tag{14}$$

where

$$\left\langle \frac{\partial E^{(2)}}{\partial t} \right\rangle = \frac{1}{2} \rho\, g \frac{\partial}{\partial x} a^2\, G(k\, h), \quad \left\langle \frac{\partial E^{(4)}}{\partial t} \right\rangle = \frac{1}{4} \rho\, g \frac{\partial}{\partial x} a^4\, k\, \omega\, Q(k\, h). \tag{15}$$

Here,

$$Q(k\, h) = \frac{9 \tanh(kh)}{16 \sinh^8(kh)} \left( k\, h + \frac{\sinh(4k\, h)}{4} \right) + \frac{2\cosh^4(k\, h) + 13\cosh^2(k\, h) - 6}{4 \sinh^4(k\, h)}, \tag{16}$$

and

$$G(k\, h) = \frac{g}{4\omega} \frac{2k\, h + \sinh(2k\, h)}{\cosh^2(k\, h)} = \frac{g}{\omega} \widetilde{G}(k\, h) \tag{17}$$

is the waves group speed $\partial\omega/\partial k$. Equation (14) can be readily integrated to yield [15]

$$G\, E(a) + \frac{k\, \omega}{g} Q\, E^2(a) = G_\infty E_\infty + \frac{k\, \omega}{g} Q_\infty\, E_\infty^2, \tag{18}$$

where $E(a) = \frac{1}{2} g\, a^2$ is a slowly variable function of $h$, and $E_\infty$, $Q_\infty = \frac{\omega}{g} G_\infty = \frac{1}{2}$ refer to infinite depth. Equation (18) serves as a starting point for studying the weakly nonlinear dynamics and statistical characteristics of random processes as waves approach the coastal zone. It is not restricted to deep or shallow water but applies to all possible depths, including intermediate ones. We use the dimensionless quantities

$$\widetilde{E} = \frac{\omega^4}{g^3} E, \quad y = k\, h, \quad \widetilde{G}(k\, h) = \frac{\omega}{g} G(k\, h), \quad \widetilde{h} = \frac{\omega^2}{g} h, \tag{19}$$

with $y$ being the solution to the equation

$$\widetilde{h} = y \tanh(y), \tag{20}$$

where $\widetilde{h}$ denotes the dimensionless depth of the fluid (as follows from the dispersion relation (11)). Now, (14) can be readily rearranged into the following form

$$\widetilde{G}\, \widetilde{E}(a) + \frac{Q}{\tanh(y)} \widetilde{E}^2(a) = \widetilde{G}_\infty \widetilde{E}_\infty + Q_\infty \widetilde{E}_\infty^2 = \frac{1}{2} (\widetilde{E}_\infty + \widetilde{E}_\infty^2). \tag{21}$$

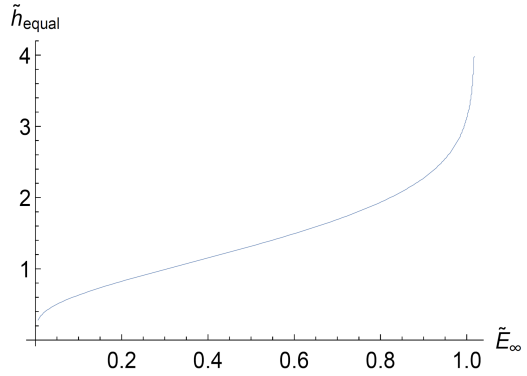


Fig. 1. Dimensionless depth $\widetilde{h}_{\text{equal}}$, at which the energies of the first and second harmonics are approximately equal, shown as a function of $\widetilde{E}_\infty$.

The energy of the first harmonic depends on the depth as follows

$$\widetilde{E}_1 \equiv \widetilde{E}(a) = \frac{\tanh(y)}{2Q}\left[-\widetilde{G} + \sqrt{\widetilde{G}^2 + \frac{2Q(\widetilde{E}_\infty + \widetilde{E}_\infty^2)}{\tanh(y)}}\right]. \tag{22}$$

The energy density of the second harmonic is given by

$$\widetilde{E}_2 = \frac{Q}{\widetilde{G}\tanh(y)}\widetilde{E}_1^2. \tag{23}$$

Figure 1 shows dimensionless depth, at which the energies of the first and second harmonics are approximately equal. In the absence of nonlinear energy transfer to higher harmonics (formally, this is the case when $Q = Q_\infty = 0$), the dimensionless energy density of the fluid volume, $\widetilde{E}_L$, varies due to changes in depth and follows from the linearized equations

$$\widetilde{E}_L = \frac{\widetilde{E}_\infty \widetilde{G}_\infty}{\widetilde{G}} = \frac{\widetilde{E}_\infty}{2\widetilde{G}}. \tag{24}$$

At small depths $\widetilde{h} \to 0$,

$$y \to \widetilde{h}^{1/2}, \qquad Q \propto \widetilde{h}^{-3}, \qquad \widetilde{G} \propto \widetilde{h}^{1/2},$$
$$\widetilde{E}_1 \propto h^{7/4}, \qquad \widetilde{E}_2 \propto h^{-1/2}. \tag{25}$$

This result corrects the conclusions of Pelinovsky [16], who predicted an energy density scaling as $\widetilde{E}_1 \propto h^{6/4}$. At large depths, $\widetilde{E} \to \widetilde{E}_\infty$. The dynamics over large depths corresponds to small surface perturbations, for which the solution almost coincides with the linear one.

### 2.2. Numerical scheme

Equations (22) and (23), together with the implicit equation (20), determine the dependence of the energies of the first and second harmonic components on the depth, while (24) describes the first harmonic in the absence of nonlinear energy transfer. The numerical solution of (20) requires some explanation. We choose the initial approximation solution as $y_0 = \widetilde{h}$ for $\tilde{h} \geq 1$ and as $y_0 = \sqrt{\widetilde{h}}$ for $\tilde{h} < 1$. Subsequent approximations are then obtained using the following iterative (recurrent) scheme

$$y_{n+1} = y_n + \varepsilon_n,$$
$$\widetilde{h} = (y_n + \varepsilon_n)\tanh(y_n + \varepsilon_n) = (y_n + \varepsilon_n)\frac{\tanh(y_n) + \tanh(\varepsilon_n)}{1 + \tanh(y_n)\tanh(\varepsilon_n)} \approx (y_n + \varepsilon_n)\frac{\tanh(y_n) + \varepsilon_n}{1 + \tanh(y_n)\varepsilon_n}. \tag{26}$$

In each iteration, $\varepsilon_n$ is determined as

$$\varepsilon_n = -\frac{1}{2}\Big(y_n + \tanh(y_n) - \widetilde{h}\tanh(y_n)\Big) + \frac{1}{2}\sqrt{\Big(y_n + \tanh(y_n) - \widetilde{h}\tanh(y_n)\Big)^2 - 4\Big(y_n\tanh(y_n) - \widetilde{h}\Big)}. \tag{27}$$

The procedure converges rapidly. Ten iterations were used in the program to obtain approximate estimates.

### 2.3. Validity of results

(i) The results are valid if $\varepsilon = ak \ll 1$. In the shallow-water case, this assumption yields the conditions

$$\widetilde{a} \ll \omega\sqrt{\frac{h}{g}} = \sqrt{\widetilde{h}}; \qquad \widetilde{E}_\infty \ll \frac{\tilde{h}}{2}, \tag{28}$$

while in the deep-water case, the following inequalities apply

$$\widetilde{a} = \frac{\omega^2}{g}a = \varepsilon \ll 1; \qquad \widetilde{E}_\infty \ll \frac{1}{2}. \tag{29}$$

(ii) The conservation equation (14) assumes weakly nonlinear processes, where a small parameter $M$ is introduced, defined as the ratio of the nonlinear term to the linear term in the momentum equation (1), both evaluated at the free surface $z = 0$,

$$M = \left| v_x \frac{\partial v_x/\partial x}{\partial v_x/\partial t}\right|_{z=0} \sim \frac{k\,a}{\tanh(k\,h)} \tag{30}$$

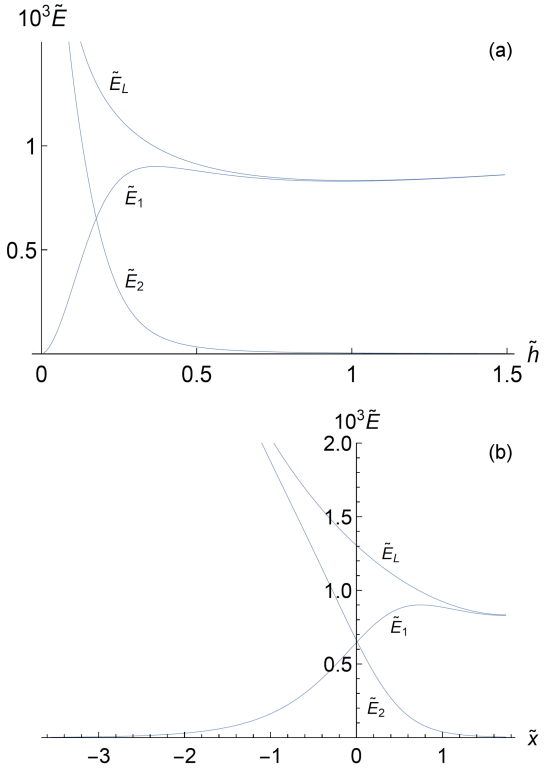


Fig. 2. The energy density of the first harmonic $\widetilde{E}_1$ and that of the second harmonic $\widetilde{E}_2$ during nonlinear dynamics ($\widetilde{E}_L$ denotes the energy during linear propagation). The total energy at infinite depth, $\widetilde{E}_\infty$, is $10^{-3}$. Panel (a) shows the energy as a function of $\widetilde{h}$, while panel (b) uses the variable $\widetilde{x} = \ln(\widetilde{h}/\widetilde{h}_{\rm equal})$.

for any $kh$ [8]. In shallow water, $M \approx \frac{a}{h}$, and the linearized theory is a very restricted approximation. In deep-water, $M$ coincides with $\varepsilon$; thus $M \approx k\,a$.

(iii) The magnitudes of the first- and second-order perturbations are smaller than the depth, so that $\widetilde{E}_1 \le \widetilde{h}^2/2$ and $\widetilde{E}_2 \le \widetilde{h}^2/2$.

(iv) Perturbation theory also requires the energy of the second harmonic to be relatively small, such that $\widetilde{E}_2 \le \widetilde{E}_1$. This condition determines the range of depths for which the solution is valid. Equation (23), together with the smallness condition reflected by $\widetilde{E}_2 \le \widetilde{E}_1$, leads to

$$Q\,\widetilde{E}_1 \le \widetilde{G}\tanh(y) \tag{31}$$

and determines the boundary depth $\widetilde{h}_{\rm equal}$ for the validity of the theory, where $\widetilde{E}_2 \approx \widetilde{E}_1$ (in numerical calculations, we demand the absolute value of $\widetilde{E}_2 - \widetilde{E}_1$ to be less than 0.01). An infinite $\widetilde{h}_{\rm equal}$ corresponds to $\widetilde{E}_\infty = 1$. For small $\widetilde{E}_\infty$, $\widetilde{h}_{\rm equal} \propto \widetilde{E}_\infty^{1/4}$. The theory is valid if $\widetilde{h} > \widetilde{h}_{\rm equal}$.

As an exemplary bottom profile, we consider

$$h = h_{\rm equal}\,\exp(x/D) \equiv h_{\rm equal}\,\exp(\widetilde{x}), \tag{32}$$

where $D$ denotes the characteristic scale of depth variation. Since the depth varies only slightly, i.e., $D \gg \lambda = 2\pi\sqrt{g\,h_{\rm equal}}/\omega$, so that

$$\widetilde{D} \gg 2\pi\sqrt{\widetilde{h}_{\rm equal}}, \tag{33}$$

where $\widetilde{D} = \frac{\omega^2}{g}\,D$ and $\widetilde{h}_{\rm equal} = \frac{\omega^2}{g}\,h_{\rm equal}$ are the dimensionless quantities. The condition (33) is consistent with the requirement that energy dissipation over one oscillation period be small, $\frac{\partial E_1/\partial t}{E_1} \ll \omega$. Indeed, taking into account $\frac{\partial E_1}{\partial t} = \frac{\partial}{\partial x}(G\,E_1)$ and (25), one arrives at

$$\frac{1}{E_1}\frac{\partial E_1}{\partial t} = \frac{9\omega\sqrt{\widetilde{h}_{\rm equal}}}{4\widetilde{D}} \ll \omega. \tag{34}$$

Figure 2 illustrates the evolution of the energy density for $\widetilde{E}_\infty$=$10^{-3}$ as the perturbation approaches the coastal zone. In panel (a), the dependence of the energy on $\widetilde{h}$ is shown, while in panel (b) the variable $\widetilde{x} = \ln(\widetilde{h}/\widetilde{h}_{\rm equal})$ is used; note that $\widetilde{h}_{\rm equal} \approx 0.175$ for $\widetilde{E}_\infty = 10^{-3}$. Strictly speaking, the results are valid only for $\widetilde{h}$>$\widetilde{h}_{\rm equal}$ ($\widetilde{x}$>0).

## 3. Propagation of random surface waves

Let us consider how the characteristics of random surface perturbations vary with depth, using the results from Sect. 2. We consider a random, stationary Gaussian process at infinite depth, such that

$$\xi = R\cos(\omega t + \varphi), \tag{35}$$

and the probability density function (PDF) of the amplitude $R$,

$$W(R) = \frac{R}{\sigma^2}\exp\left(-\frac{R^2}{2\sigma^2}\right). \tag{36}$$

The probability density functions (PDFs) for the phase $\varphi$ and for the surface perturbation $\xi$ are given by the following expressions

$$W(\varphi) = \frac{1}{2\pi},$$
$$W(\xi) = \frac{1}{\sqrt{2\pi\sigma^2}}\exp\left(-\frac{\xi^2}{2\sigma^2}\right). \tag{37}$$

As the wave approaches the coastal zone, the process remains stationary, with the amplitude and phase depending only weakly on the depth $h$, so that $\xi(h) = a(h)\cos(\omega t + \varphi(h))$. The leading-order form of the energy conservation law reads as (in fact, it is a rearranged form of (18))

$$\frac{g\,a^2}{2}G + \left(\frac{g\,a^2}{2}\right)^2\frac{k\omega}{g}Q = \frac{g\,R^2}{2}\frac{g}{2\omega} + \left(\frac{g\,R^2}{2}\right)^2\frac{\omega^3}{2g^2}. \tag{38}$$

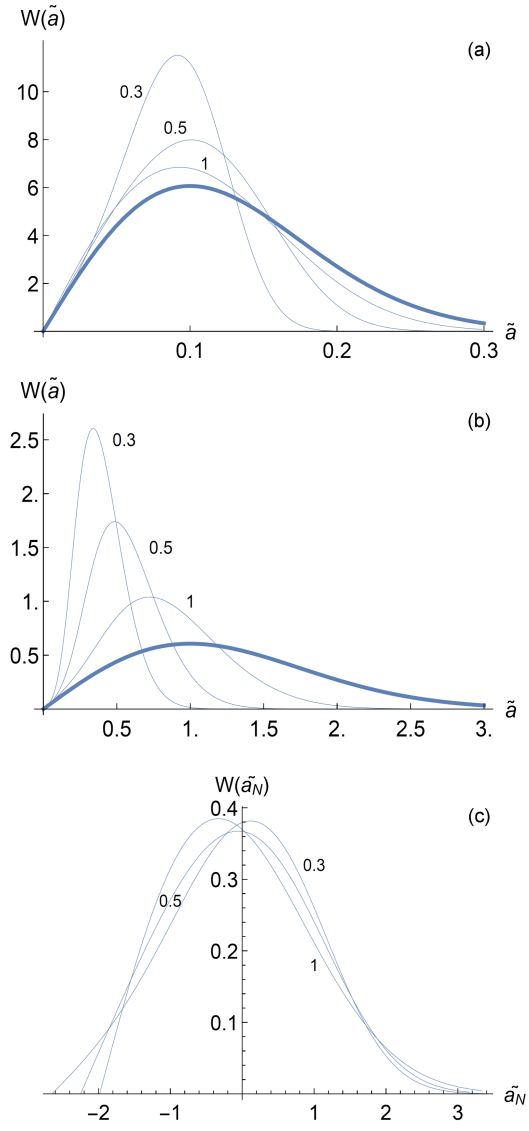


Fig. 3. (a, b) PDFs $W(\widetilde{a})$ for different values of $\widetilde{h} = 0.3,\ 0.5,\ 1$ and for (a) $\widetilde{\sigma} = 0.1$, (b) $\widetilde{\sigma} = 1$. The thick line represents the Rayleigh distribution given by (36). (c) PDF $W(\widetilde{a}_N)$ of the normalized distribution for $\widetilde{\sigma} = 0.1$.

This allows $R$ to be expressed in terms of $a$ as

$$R = \sqrt{-\frac{g^2}{\omega^4} + \frac{\sqrt{g\left(g^3 + 4a^2\,G\omega^5 + 2a^4\,k\,\omega^6\,Q\right)}}{\omega^4}}. \tag{39}$$

The PDF $W(a) = W(R)\frac{\mathrm{d}R}{\mathrm{d}a}$ takes the following form

$$W(a) = \frac{2a\,g\,\omega\,(G + a^2\,k\,\omega\,Q)}{\sigma^2\sqrt{g^4 + 2a^2\,g\,\omega^5(2G + a^2\,k\,\omega\,Q)}} \times \exp\left(\frac{g^2 - \sqrt{g^4 + 2\,a^2\,g\omega^5\left(2G + a^2\,k\,\omega\,Q\right)}}{2\omega^4\sigma^2}\right) \tag{40}$$

(this function also depends on $\widetilde{h}$ through $G$ and $Q$, see (15)). Using the dimensionless variables given in (19) and also $\widetilde{\sigma} = \frac{\omega^2}{g}\sigma$, the PDF $W(\widetilde{a}) = \frac{g}{\omega^2}W(a)$ for the dimensionless amplitude $\tilde{a}$ takes the form

$$W(\widetilde{a}) = \frac{2(\widetilde{G}\,\widetilde{a} + \widetilde{a}^3\,Q\,y/\widetilde{h})}{\widetilde{\sigma}^2\sqrt{1 + 4\,\widetilde{a}^2\,\widetilde{G} + 2\widetilde{a}^4\,y\,Q/\widetilde{h}}} \times \exp\left(-\frac{\sqrt{1 + 4\widetilde{a}^2\,\widetilde{G} + 2\widetilde{a}^4\,y\,Q/\widetilde{h}} - 1}{2\,\widetilde{\sigma}^2}\right). \tag{41}$$

In the shallow-water limit,

$$W(\widetilde{a}) \approx \frac{\widetilde{a}\sqrt{2Q(\widetilde{h})}}{\widetilde{h}^{1/4}\widetilde{\sigma}^2}\exp\left(-\frac{\widetilde{a}^2\sqrt{Q(\widetilde{h})}}{\sqrt{2}\widetilde{h}^{1/4}\widetilde{\sigma}^2}\right). \tag{42}$$

The mean value $M[\widetilde{a}]$ and the variance $D[\widetilde{a}]$ are determined using

$$M[\widetilde{a}] = \int_0^\infty \mathrm{d}a\ W(\widetilde{a})\,\widetilde{a},$$
$$D[\widetilde{a}] = \int_0^\infty \mathrm{d}a\ W(\widetilde{a})\Big(\widetilde{a} - M[\widetilde{a}]\Big)^2. \tag{43}$$

Figure 3 shows the PDFs of $\widetilde{a}$ and the PDFs of the normalized amplitude $\widetilde{a}_N = \widetilde{a} - M[\widetilde{a}]/\sqrt{D[\widetilde{a}]}$ (where $M[\widetilde{a}_N] = 0$, $D[\widetilde{a}_N] = 1$) for different values of $\widetilde{h}$ and $\widetilde{\sigma}$. In Fig. 3c, the corresponding curves of the PDF $W(\widetilde{a}_N)$ at $\widetilde{\sigma} = 1$ are almost indistinguishable for $\widetilde{h} = 0.3$, 0.5, and 1.

Let $W(\widetilde{a})$ attain its maximum at $\widetilde{a}_{\max}$. It is easy to show that, for small $\widetilde{h}$,

$$\widetilde{a}_{\max} \approx \frac{\widetilde{\sigma}\,\widetilde{h}^{-1/8}}{\sqrt[4]{2Q(\widetilde{h})}} \propto \widetilde{h}^{7/8},$$
$$W(\widetilde{a}_{\max}) \approx \frac{4\sqrt{2}\,\widetilde{h}^{-1/8}\mathrm{e}^{-1/2}}{\widetilde{\sigma}}\sqrt[4]{Q(\widetilde{h})} \propto \widetilde{h}^{-7/8}, \tag{44}$$

The mean values of $\widetilde{a}$ and $\widetilde{a}^2$, as well as the variance of $\widetilde{a}$ at small $\widetilde{h}$, are approximately estimated as

$$M[\widetilde{a}] \approx \frac{\widetilde{\sigma}\,\widetilde{h}^{-1/8}}{\sqrt[4]{2Q(\widetilde{h})}} \approx \widetilde{a}_{\max} \propto \widetilde{h}^{7/8},$$
$$M[\widetilde{a}^2] \approx \frac{2\widetilde{\sigma}^2\,\widetilde{h}^{-1/4}}{\sqrt{2Q(\widetilde{h})}} \propto \widetilde{h}^{7/4},$$
$$D[\widetilde{a}] = M[\widetilde{a}^2] - M^2[\widetilde{a}] = \frac{\widetilde{\sigma}^2\,\widetilde{h}^{-1/4}}{\sqrt{2Q(\widetilde{h})}} \propto \widetilde{h}^{7/4}. \tag{45}$$

The mean $M[\widetilde{a}]$ and the variance $D[\widetilde{a}]$ decrease as the coastal zone is approached, i.e., when $h$ geets smaller. This reflects the damping of the main harmonic and the transfer of energy to higher harmonics. For large $\widetilde{h}$, $\widetilde{a} \to R$, $y \to \widetilde{h}$, $\widetilde{G} \to 0.5$, $Q \to 0.5$, and moreover, the probability density function (41) tends to the Rayleigh form when expressed in terms of the dimensionless variable $\widetilde{R} = \frac{\omega^2}{g}R$, for which $W(\widetilde{R})$ attains its a maximum at $\widetilde{R}_{\max} = \widetilde{\sigma}$; thus

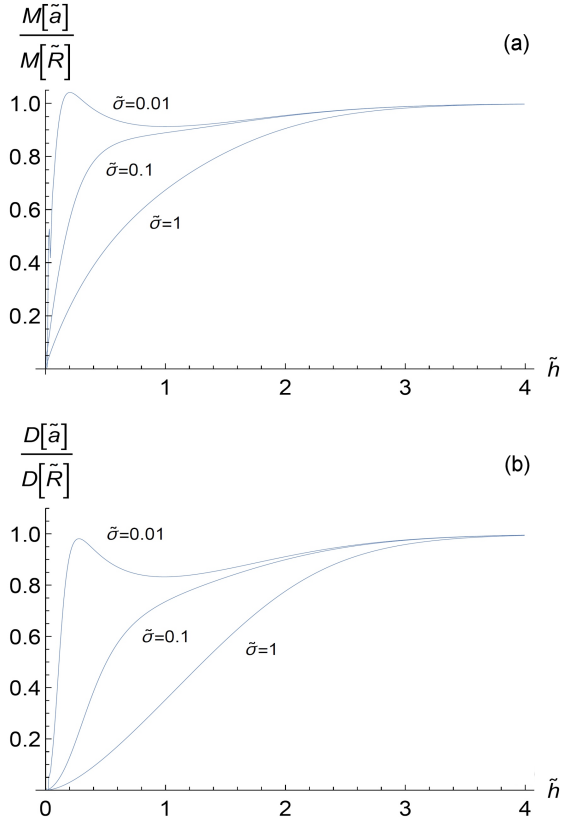


Fig. 4. Dimensionless mean value $M[\widetilde{a}]/M[\widetilde{R}]$ and variance $D[\widetilde{a}]/D[\widetilde{R}]$ normalized by their values at infinite depth, shown as functions of $\widetilde{h}$. The curves correspond to different values of $\widetilde{\sigma} = 0.01,\ 0.1,\ 1$.

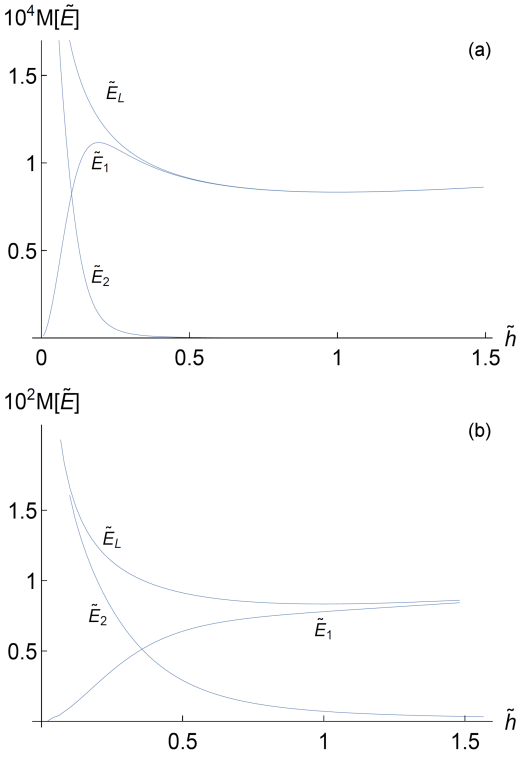


Fig. 5. Mean energy of the first harmonic $M[\widetilde{E}_1]$ and that of the second harmonic $M[\widetilde{E}_2]$ during nonlinear dynamics ($M[\widetilde{E}_L]$ denotes the mean energy during linear propagation). The total mean energy at the infinite depth, $\widetilde{E}_\infty = \widetilde{\sigma}^2$, is equal to (a) $10^{-4}$ and (b) $10^{-2}$.

$$W(\widetilde{R}) = \frac{\widetilde{R}}{\widetilde{\sigma}^2}\exp\left(-\frac{\widetilde{R}^2}{2\widetilde{\sigma}^2}\right),$$
$$M[\widetilde{R}] = \sqrt{\frac{\pi}{2}}\widetilde{\sigma}, \qquad M[\widetilde{R}^2] = 2\widetilde{\sigma}^2,$$
$$W(\widetilde{R}_{\max}) = \frac{\mathrm{e}^{-1/2}}{\widetilde{\sigma}}. \tag{46}$$

The PDF $W(\widetilde{a})$ almost coincides with the Rayleigh probability distribution at depth $\widetilde{h} = 5$ for standard deviation $\widetilde{\sigma} = 1$.

For small $\widetilde{\sigma}$, maxima appear in the curves $M[\widetilde{a}]/M[\widetilde{R}]$ and $D[\widetilde{a}]/D[\widetilde{R}]$ (see, for example, $\widetilde{\sigma} = 10^{-2}$ in Fig. 4). This reflects the strong adherence of the first-harmonic energy $\widetilde{E}_1$ to the linear energy $\widetilde{E}_L$ for small-amplitude surface perturbations far from the coastal zone, as discussed in Sect. 2 (see Fig. 2). The mean values $M[\widetilde{E}_1]$, $M[\widetilde{E}_2]$, $M[\widetilde{E}_L]$ for different values of $\widetilde{E}_\infty$ as functions of $\widetilde{h}$ are presented in Fig. 5. The curves in Fig. 5a also confirm the strong adherence of the first harmonic to the linear curve down to a certain limiting depth as the small-amplitude perturbations approach the coastal zone.

The solutions for the case $\widetilde{\sigma} = 1$ are particularly illustrative. Nevertheless, the results are valid only under the condition that perturbations far from the coastal zone are small, that is, $\widetilde{\sigma}^2 = \frac{1}{2}M[\widetilde{R}^2] \ll 1$.

## 4. Conclusions

This study focuses on weakly nonlinear effects during the propagation of a random, stationary Gaussian waves toward the coastal zone. Surface gravity waves propagating over a region of a slightly varying depth are considered. The results may be useful for calculating parameters of surface disturbances caused by bottom movements or, for example, explosions, as well as in situations where several statistically independent processes are superimposed, and their collective effect brings the total response closer to Gaussian noise. In accordance with the central limit theorem, when many independent, identically distributed random processes are superimposed — each with its own PDF (not necessarily normal) and finite mean and variance, — the PDF of their sample mean approaches the normal distribution as the sample size becomes

large. In this paper, (18) forms a foundation for the analysis of the weakly nonlinear dynamics and the statistical properties of random waves as they propagate toward the coastal zone. It is applicable to the full range of water depths, from deep to shallow, including intermediate depths.

Sections 2 and 3 represent the theory and results of numerical calculations, namely:

(i) Evaluation of the limiting depth (at which the energies of the first and second harmonic components become equal) as a function of the total wave energy far from the coastal zone;

(ii) Qualitative and quantitative analysis of the propagation of the first and second harmonics over weakly varying depth, in particular for exponential bottom profile;

(iii) Derivation of the probability density function (PDF) for the amplitude of random Gaussian waves as a function of the dimensionless depth and the variance of the perturbation amplitude far from the coastal zone. Evaluation of the mean value $M[\widetilde{a}]$ and the variance $D[\widetilde{a}]$ of the dimensionless amplitude as functions of depth and the variance of the perturbation amplitude far from the coastal zone;

(iv) It is inferred that, as the coastal zone is approached, nonlinear processes intensify abruptly when the variance of the dimensionless total wave energy at infinite depth, $\widetilde{E}_\infty$, is less than $4 \times 10^{-3}$, whereas for larger values of $\widetilde{E}_\infty$, the evolution of nonlinear effects is gradual. The numerical code enables the analysis of cases with strong (deep-water) and weak (shallow-water) dispersion, as well as the transition regime between them. For small $\widetilde{E}_\infty$, the results indicate a strong adherence of the first-harmonic energy $\widetilde{E}_1$ to the linear energy curve $\widetilde{E}_L$, beginning from a certain water depth. According to the numerical evaluations, $\widetilde{E}_1$ attains a local maximum $\widetilde{E}_{\max}$ at depth $\widetilde{h}_{\max}$ when $\widetilde{E}_\infty \leq 4 \times 10^{-3}$. For larger values of $\widetilde{E}_\infty$, $\widetilde{E}_1$ becomes a monotonically increasing function of $\widetilde{h}$. We may therefore conditionally assume that strong adherence occurs for $\widetilde{h} > \widetilde{h}_{\max}$. Numerical results for $\widetilde{h}_{\max}$ and $\widetilde{E}_{1,\max}/\widetilde{E}_\infty$ as functions of $\widetilde{E}_\infty$ are shown in Fig. 6. Evidently, $\widetilde{h}_{\max} > \widetilde{h}_{\text{equal}}$ for all values of $\widetilde{E}_\infty$.

The abrupt intensification of nonlinear behavior in perturbations contrasts with the slow accumulation of nonlinear effects that is typical in acoustics of fluids. The dynamics of surface gravity waves depends only on the parameters $\widetilde{E}_\infty$ and $\widetilde{h}$. There is a complete analogy with the transfer of energy from the fundamental harmonic with amplitude $a_{1,\infty}$ and frequency $\omega_1$ to the higher harmonic with amplitude $a_{2,\infty}$ and frequency $\omega_2$ when the condition $a_{1,\infty}\omega_1 = a_{2,\infty}\omega_2$ is satisfied.

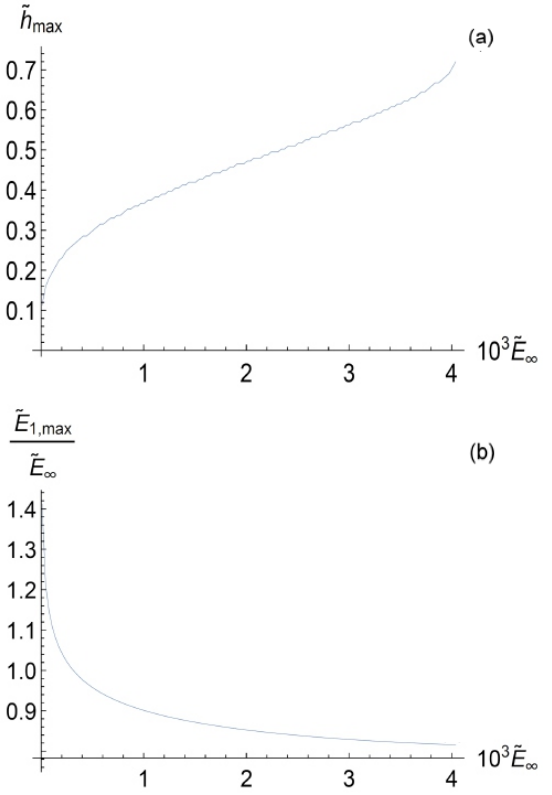


Fig. 6. (a) The results of $\widetilde{h}_{\max}$ corresponding to the maximum of $\widetilde{E}_1(\widetilde{h})$ shown as a function of $\widetilde{E}_\infty$. For $\widetilde{h} > \widetilde{h}_{\max}$, the dynamics is nearly linear. (b) The ratio $\widetilde{E}_{1,\max}/\widetilde{E}_\infty$ shown as a function of $\widetilde{E}_\infty$.

This behavior may be explained by a determining parameter, namely the shock-formation distance in a nonlinear, nondispersive medium, which is proportional to $(\omega a)^{-1}$. In this respect, the dependence of the energy density transform solely on the product $\omega\, a_\infty$ is in good agreement with our analysis. Under the assumptions of theory, this circumstance also holds true when dispersion in deep water is taken into account.

The coastal water layer is of particular interest because it is a type of system in which a wide range of nonlinear phenomena are observed. A promising approach at present is the spectral method of analysis, which treats waves as a complex process resulting from the superposition of a large number of sinusoidal waves along with the summation of wave–wave interactions for all possible pairs. The analytical approach is often complemented by numerical simulations. In the study [14], unknown coefficients in the power series expansions of the velocity potential and wave elevation over a region of constant depth are determined so that second-order dynamic and kinematic boundary conditions are satisfied. For this purpose, the author employed symbolic computation. The results are readily applicable to the study of irregular wave elevations composed of $N$ ($N \geq 2$) linear components.

The samples of simulated irregular wave elevations presented in [14] are constructed using linear components with prescribed amplitudes, incommensurate frequency realizations of the JONSWAP spectrum, and randomly selected phases of each linear component. A body of water of constant depth is considered.

This study has obvious limitations. One of them is the stationary transfer of energy from the first harmonic to the second harmonic; therefore, it is restricted to the fundamental and second harmonics of the wave elevation. This simplification leads to simple analytical formulas and allows us to make certain assessments concerning the nature of the nonlinear propagation of random waves over variable water depth, depending on the total mean energy far from the coastal zone. Furthermore, the wavenumber is treated as a one-dimensional quantity. The study does not attempt to describe the full diversity of statistical phenomena, but instead relies on reasonable assumptions, in particular, on the use of a continuous probability density function (PDF) for the wave elevation amplitude.

## References


[1] G.B. Airy, *Tides and Waves, Encyclopaedia Metropolitana*, 1841.

[2] G.G. Stokes, *Trans. Camb. Phil. Soc.* **8**, 441 (1847).

[3] D.J. Korteweg, G. de Vries, *Philos. Mag.* **39**, 422 (1895).

[4] O.M. Phillips, *J. Fluid Mech.* **2**, 417 (1957).

[5] J.W. Miles, *J. Fluid Mech.* **3**, 185 (1957).

[6] R.G. Dean, R.A. Dalrymple, *Water Wave Mechanics for Engineers and Scientists*, World Scientific, Singapore 1991.

[7] L.H. Holthuijsen, *Waves in Oceanic and Coastal Waters*, Cambridge University Press, Cambridge 2007.

[8] C.C. Mei, M. Stiassnie, D.K.-P. Yue, *Theory and Applications of Ocean Surface Waves*, World Scientific, Singapore 2005.

[9] G.B. Whitham, *Linear and Nonlinear Waves*, Wiley-Interscience, New York 1974.

[10] P.A. Madsen, H.B. Bingham, H. Liu, *J. Fluid Mech.* **462**, 462 (2002).

[11] L.D. Landau, E.M. Lifshitz, *Fluid Mechanics*, Pergamon Press, New York 1959.

[12] L.A. Ostrovsky, E.N. Pelinovskiy, *Izv. Atmos. Oceanic Phys.* **6**, 552 (1970).

[13] L.A. Ostrovsky, K. Gorshkov, in: *Nonlinear Science at the Dawn of the 21th Century*, ed. by P.L.Christiansen, M.P.Sorensen, A.C. Scott, Springer-Verlag, Berlin 2000, p. 47.

[14] J.F. Dalzell, *Appl. Ocean Res.* **21**, 105 (1999).

[15] S.K. Rosenfeld, *Izv. Atmos. Oceanic Phys.* **19**, 1011 (1983).

[16] E.N. Pelinovsky, *Nonlinear Dynamics of Tsunami Waves*, Institute of Applied Physics, USSR Academy of Sciences, Gor'kii 1982 (in Russian).